Journal of Catalysis 342 (2016) 151–157

Contents lists available at ScienceDirect

Journal of Catalysis

journal homepage: www.elsevier.com/locate/jcat

Coupling MOF-based photocatalysis with Pd catalysis over Pd@MIL-100(Fe) for efficient N-alkylation of amines with alcohols under visible light

Dengke Wang, Zhaohui Li *

Research Institute of Photocatalysis, State Key Laboratory of Photocatalysis on Energy and Environment, College of Chemistry, Fuzhou University, Fuzhou 350002, People's Republic of China

ARTICLE INFO

Article history:
Received 19 June 2016
Revised 26 July 2016
Accepted 27 July 2016

Keywords:
Pd nanoparticles
MIL-100(Fe)
Double-solvent impregnation
Multifunctional catalyst
Light-induced N-alkylation reaction

ABSTRACT

Pd nanoparticles with an average size of 1.7 nm confined inside a MIL-100(Fe) cavity (Pd@MIL-100(Fe)) were prepared via double-solvent impregnation combined with a photoreduction process. Due to efficient coupling of photocatalytic dehydrogenation and Pd-based hydrogenation, the resultant Pd@MIL-100(Fe) showed significantly superior performance in light-induced N-alkylation of amines with alcohols over Pd/MIL-100(Fe), in which larger Pd nanoparticles (6–12 nm) deposited on the external surface of MIL-100(Fe) were prepared via a conventional single-solvent impregnation followed by a similar photoreduction process. Kinetic studies and controlled experiments revealed that the whole N-alkylation reaction is limited by the photocatalytic alcohol-to-aldehyde dehydrogenation reaction. This is the first demonstration of light-induced N-alkylation of amines by alcohols over M/MOFs nanocomposites and also highlights the great potential of using M/MOFs nanocomposites as multifunctional catalysts for light-induced organic syntheses.

1. Introduction

As important chemicals, N-alkyl amines are important building blocks for the generation of agrochemicals, pharmaceuticals, and bioactive molecules [1,2]. An attractive route for the production of N-alkyl amines is the direct alkylation of amines with alcohols as alkylating agents, since such a reaction has a high atom efficiency and produces water as the only byproduct [3–6]. Until now, a variety of catalysts, mostly Ru- and Ir-based homogeneous catalysts, as well as some noble metal nanoparticle-doped heterogeneous catalysts, have been developed for N-alkylation of amines with alcohols [7–10]. Unfortunately, the catalytic performance of these systems is far from satisfactory. Usually the homogeneous systems suffer from limited reusability and indispensable use of co-catalysts [11,12], while most of the heterogeneous systems are used under harsh conditions, in which overalkylation occurs. In addition, deterioration of the performance of metal-nanoparticle-based heterogeneous systems is unavoidable due to the aggregation of metal nanoparticles [13]. Therefore, the development of stable and highly efficient heterogeneous catalytic systems for N-alkylation reactions under mild conditions, in particular under solar light irradiation, is highly desirable.

It is widely accepted that the N-alkylation of amines with alcohols follows a hydrogen autotransfer mechanism containing three consecutive catalytic steps: dehydrogenation of alcohols to aldehydes, condensation of aldehydes with amines to imines, and hydrogenation of imines to N-alkyl amines [3–6,14–17]. To realize these consecutive steps in one pot, multifunctional catalysts containing different catalytically active sites are required. Recently, TiO_2-supported Pd, Au, and Cu–Mo nanoparticles have been reported to show activity in this one-pot alkylation reaction under UV light irradiation [18–20]. Although the light-induced alkylation of amines with alcohols is quite appealing, since the reaction conditions are mild and the process requires no co-catalysts, these metal/TiO_2 nanocomposites only take effect under UV irradiation and the aggregation of metal nanoparticles during the reactions, which would deteriorate their activity, cannot be avoided. Additionally, the morphology of the metal nanoparticles plays an important role in their catalytic performance. Small nanoparticles are usually more active, since they contain more coordinated unsaturated sites, which are the actual active sites for catalytic reaction [18]. However, size-controllable preparations of metal nanoparticles on the surfaces of semiconductors are usually challenging, since aggregation of these small nanoparticles occurs readily due to their high surface energy.

The employment of the nanopores in porous materials as nanoreactors for direct growth of nanoparticles is a widely adopted

---

* Corresponding author. Fax: +86 591 83779260.
E-mail address: zhaohuili1969@yahoo.com (Z. Li).

http://dx.doi.org/10.1016/j.jcat.2016.07.021
0021-9517/

and effective strategy for obtaining nanoparticles with controllable size [21–28]. Metal–organic frameworks (MOFs), a class of hybrid materials with highly ordered uniform nanopores, can provide well-defined microenvironments for controllable growth of nanoparticles [29–44]. Although still in their infancy, metal/MOFs nanocomposites with metal nanoparticles encapsulated inside the cavity have already shown promise in heterogeneous catalysis [45–54]. Photocatalysis is a unique kind of heterogeneous catalysis that involves the use of a light source [55–57]. Recently, MOFs have emerged as a new type of promising photocatalysts due to their tunable light absorption and the ability to organize different functional components in an individual MOF material [58–64]. In addition, the highly crystalline nature of MOFs ensures rapid electron and energy transfer from the photoexcited MOFs to the active sites for a variety of photocatalytic reactions [65–70].

Here, we report the preparation of Pd nanoparticles encapsulated inside the MIL-100(Fe) cavity (Pd@MIL-100(Fe)) via double-solvent impregnation combined with a photoreduction process and its application for light-induced N-alkylation of amines with alcohols. As compared with Pd/MIL-100(Fe), in which larger Pd nanoparticles were deposited on the surface of MIL-100(Fe), Pd@MIL-100(Fe) showed superior catalytic activity and higher stability. For the first time, this work demonstrates the use of the nanopores in MOFs for controllable growth of metal nanoparticles encapsulated inside MOFs as a way to realize a highly efficient and stable alkylation of amines via successful coupling of the MOF-based photocatalysis and metal NPs-based hydrogenation.

2. Experiments

2.1. Preparations

All the reagents were commercially available and used without further purification. MIL-100(Fe) was prepared following the procedures described in the literature with slight modifications [71–74]. Typically, iron(III) nitrate nonahydrate (484 mg, 1.2 mmol) and 1,3,5-benzenetricarboxylic acid (210 mg, 1.0 mmol) were dissolved in deionized water (5 mL). Then the resulting solution was stirred, transferred to a Teflon autoclave liner, and sealed to heat at 180 °C for 12 h. The obtained yellow solid was recovered by filtration and washed several times with deionized water and methanol. The synthesized MIL-100(Fe) was finally dried overnight at 60 °C in an oven.

Pd@MIL-100(Fe) was prepared by a double-solvent impregnation approach combined with a photoreduction process. The double-solvent impregnation approach was first developed by Xu et al. for the preparation of Pt@MIL-101(Cr) and AuNi@MIL-101(Cr) [75,76]. For the impregnation, 100 mg of activated MIL-100(Fe) was suspended in 20 mL of dry *n*-hexane and 0.08 mL of an aqueous solution containing $PdCl_2(CH_3CN)_2$ (2.46 mg, 1 wt.% Pd) was added dropwise within 15 min under vigorous stirring. After the mixture was stirred for 2 h, the solid was isolated from the supernatant by decanting, washed with ethanol, and dried under vacuum. The as-obtained solid product was then suspended in degassed anhydrous methanol and was irradiated under visible light for 3 h. The resultant sample was filtered, washed with methanol, and dried overnight at 60 °C in an oven.

For comparison, Pd/MIL-100(Fe) was synthesized employing the direct photoreduction method via a conventional single-solvent impregnation process. A quantity of 0.08 mL of an aqueous solution of $PdCl_2(CH_3CN)_2$ (2.46 mg, 1 wt.% Pd) was added to the degassed anhydrous methanol (5 mL) containing 100 mg of MIL-100(Fe) under N_2. The as-obtained suspension was irradiated under visible light for 3 h. The resultant solid was filtered, washed with methanol, and dried overnight at 60 °C in an oven. Pd/Fe_2O_3 and Pd/TiO_2 were prepared similarly to Pd/MIL-100(Fe) except that UV light (254 nm) was used for the preparation of Pd/TiO_2.

2.2. Characterizations

X-ray diffraction (XRD) patterns were collected on a D8 Advance X-ray diffractometer (Bruker, Germany) with Cu Kα radiation. The accelerating voltage and the applied current were 40 kV and 40 mA, respectively. Data were recorded at a scanning rate of $0.02° \ 2\theta \ s^{-1}$ in the 2θ range of 5–30°. UV–visible diffuse reflectance spectra (UV-DRS) of the powders were obtained with $BaSO_4$ used as a reflectance standard. BET surface area was determined on an ASAP 2020M apparatus (Micromeritics Instrument Corp., USA). The samples were degassed under vacuum at 150 °C for 10 h and then measured at −196 °C. The transmission electron microscopy (TEM) and high-resolution transmission electron microscopy (HRTEM) images were obtained on a JEOL model JEM 2010 EX instrument. X-ray photoelectron spectroscopy (XPS) measurements were performed on a PHI Quantum 2000 XPS system (PHI, USA). Inductively coupled optical emission spectrometry (ICP-OES) was performed on Optima 8000 (PerkinElmer). Before the ICP-OES experiment, the solid sample was digested in a mixture of HNO_3 and Milli-Q water.

2.3. Catalytic reactions

The N-alkylation reaction was performed in a sealed reaction tube under visible light irradiation. The catalyst (10 mg), amine (0.1 mmol), and alcohol (3 mmol) were suspended in acetonitrile (CH_3CN, 2 mL) and the resultant mixture was degassed and saturated with N_2 to remove any dissolved O_2 before the reaction. The reaction was performed under irradiation by a 300 W Xe lamp equipped with a UV-cut filter to remove all irradiation with wavelengths less than 420 nm and an IR-cut filter to remove all irradiation with wavelengths greater than 800 nm. After the reaction, the reaction mixture was filtered through a porous membrane (20 μm in diameter) and the products were analyzed by GC-MS and GC-FID (Shimadzu GC-2014) equipped with an HP-5 capillary column.

Photocatalytic dehydrogenation of benzyl alcohol was conducted in a sealed reaction tube containing Pd@MIL-100(Fe) (10 mg), benzyl alcohol (0.1 mmol), and CH_3CN (2 mL).

Hydrogenation of N-benzylideneaniline with H_2 was carried out in a reaction tube containing Pd@MIL-100(Fe) (10 mg), N-benzylideneaniline (0.1 mmol), benzyl alcohol (3 mmol), and CH_3CN (2 mL).

Hydrogenation of N-benzylideneaniline over H_2-pretreated Pd@MIL-100(Fe) was carried out in a Schlenk tube. Pd@MIL-100(Fe) was first activated and treated with H_2 for 1 h at 120 °C in the tube. Then the H_2 was removed, followed by filling the tube with N_2. Finally, CH_3CN solution (2 mL) containing N-benzylideneaniline (0.1 mmol) was added and stirred under room temperature.

The catalytic reaction between aniline and benzaldehyde was carried out in a tube containing Pd@MIL-100(Fe) (10 mg), aniline (0.1 mmol), benzaldehyde (0.5 mmol), and CH_3CN (2 mL).

The deuterium-labeling experiments were conducted using benzyl alcohol and benzyl alcohol-α,α-d_2 as alkylating agent. The kinetic isotope effect (KIE) is defined as k_H/k_D, in which k_H and k_D are the rate constants for the alkylation reactions carried out over benzyl alcohol and benzyl alcohol-α,α-d_2, respectively.

3. Results and discussion

MIL-100(Fe) was chosen as the host matrix to encapsulate Pd nanoparticles due to its good resistance to water and organic solvents [71–74]. The as-obtained product shows similar XRD patterns and comparable surface area (2021 m^2/g) to those reported previously (Figs. 1a and S1a), confirming the formation of MIL-100(Fe) with high quality. Pd@MIL-100(Fe) was prepared via a double-solvent method followed by a photoreduction approach. For the impregnation process, activated MIL-100(Fe) was suspended in a large amount of dry n-hexane, followed by dropwise addition of $PdCl_2(CH_3CN)_2$ aqueous solution with a volume less than the pore volume of MIL-100(Fe) under vigorous stirring. It is believed that the hydrophobic hexane will cover the external surface, which ensures the diffusion of hydrophilic Pd precursors into the pores of MIL-100(Fe) via capillary force. The following photoreduction resulted in the formation of Pd@MIL-100(Fe). A similar double-solvent impregnation process was first developed by Xu et al. to encapsulate Pt and AuNi nanoparticles inside the cavity of MIL-101(Cr) [75,76]. As compared with the reduction process using strong reducing agents such as H_2 and $NaBH_4$, the current photoreduction is milder and green, since no extra reducing agent is required, which is more favorable for preserving the MOFs framework.

The as-prepared Pd@MIL-100(Fe) shows XRD patterns similar to those of the parent MIL-100(Fe), indicating that the framework of MIL-100(Fe) is well preserved (Fig. 1a). Although no characteristic diffractions for Pd were detected in XRD patterns, XPS results confirm the existence of Pd by showing two peaks at 335.4 and 340.7 eV, corresponding to $Pd^0 3d_{5/2}$ and $Pd^0 3d_{3/2}$, respectively (Fig. 1b) [77]. TEM images show that the surface of Pd@MIL-100(Fe) is smooth, confirming that there is no Pd deposition on the external surface of MIL-100(Fe) (Fig. 1c). The HRTEM image reveals that Pd nanoparticles with size *ca.* 1.7 nm are highly dispersed in Pd@MIL-100(Fe), indicating that Pd nanoparticles have been confined in the pores of MIL-100(Fe) (Figs. 1d and S2). The lattice fringe of 0.224 nm matches that of the (111) plane of face-centered cubic Pd (inset in Fig. 1d) [77]. The amount of encapsulated Pd in Pd@MIL-100(Fe) was determined to be 0.99 wt.% by ICP-OES, almost identical to the amount of Pd added (1 wt.% Pd). These demonstrate that the double-solvent approach can effectively confine the Pd nanoparticles to the MIL-100(Fe) cavities. The encapsulation of Pd nanoparticles inside the cavity of MIL-100(Fe) leads to a decrease of the specific surface area from the original 2021 $m^2\,g^{-1}$ for MIL-100(Fe) to 1562 $m^2\,g^{-1}$ for Pd@MIL-100(Fe) (Fig. S1b). The UV–vis DRS spectrum of the Pd@MIL-100(Fe) shows enhanced absorption in the 200–550 nm region as compared with pristine MIL-100(Fe), with the adsorption edge extending to around 650 nm (Fig. 2).

To study the catalytic performance of the as-prepared Pd@MIL-100(Fe) for N-alkylation of amines with alcohols under visible light irradiation, the reaction between aniline (1a) and benzyl alcohol (2a) was chosen and was carried out in CH_3CN (Table 1). It was found that only negligible N-benzylideneaniline was obtained in the absence of Pd@MIL-100(Fe) or without visible light (Table 1, entries 1 and 2). In the presence of Pd@MIL-100(Fe), the N-alkylation of aniline with benzyl alcohol proceeded smoothly and the aniline/benzyl alcohol mole ratio played an important role in the reaction (Table 1, entries 3–8). Among all the aniline/benzyl alcohol ratios investigated, the catalytic system containing aniline and benzyl alcohol in a ratio of 1:30 gave the best performance, showing the highest conversion of aniline at 88% and a selectivity to N-benzylaniline (3a) at 76% after being irradiated for 24 h (Table 1, entry 6). By-products such as N-benzylideneaniline (3b) and benzaldehyde were also produced, but no overalkylated tertiary amine was detected. A prolonged reaction time of 32 h led to an almost quantitative transformation of aniline (>99%) at an increased selectivity to 3a (86%, Table 1, entry 9). Pd was essential to the reaction, because no activity was observed over MIL-100(Fe) under typical reaction conditions (Table 1, entry 10). The filtrate reaction revealed that no further reaction occurred after Pd@MIL-100(Fe) was removed from the reaction system (Table 1, entry 11). These results demonstrated that the alkylation of aniline with benzyl alcohol was efficiently catalyzed by Pd@MIL-100(Fe) under visible light irradiation. To further confirm that the current reaction is really photoactivated, action spectrum analyses for amine alkylation over Pd@MIL-100(Fe) have been studied. The conversion of aniline over Pd@MIL-100(Fe) is observed to depend strongly on the wavelength in a manner that correlates with their absorption intensities in the visible light region, indicating that the amine alkylation reaction over Pd@MIL-100(Fe) is truly induced by visible light (Fig. 3). Pd@MIL-100(Fe) showed superior performance for

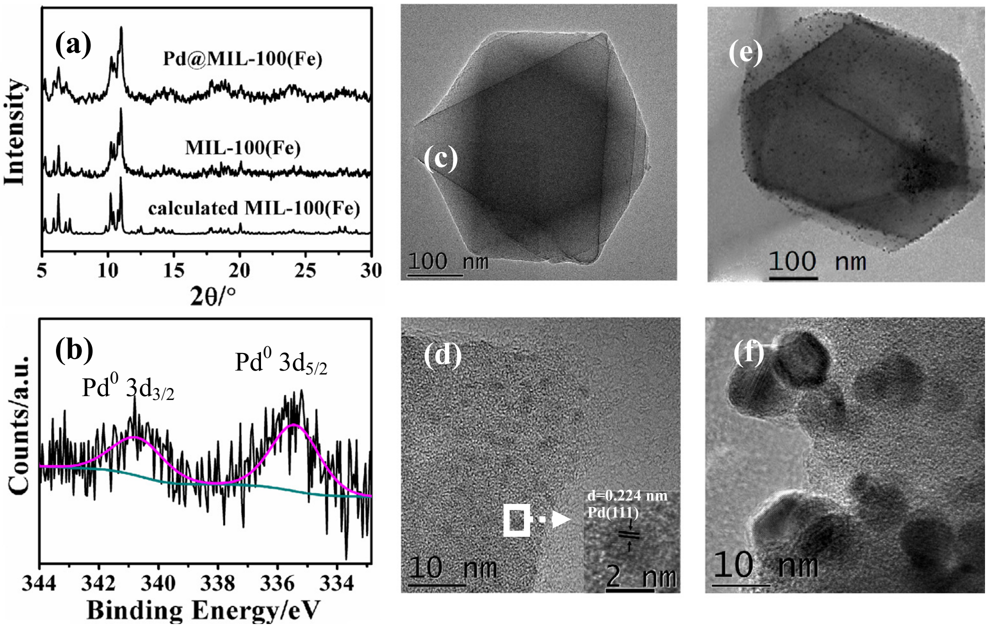

Fig. 1. (a) XRD patterns of Pd@MIL-100(Fe), MIL-100(Fe), and calculated MIL-100(Fe); (b) XPS spectrum of Pd@MIL-100(Fe) in Pd3*d* region; (c) TEM and (d) HRTEM images of Pd@MIL-100(Fe); (e) TEM and (f) HRTEM images of Pd/MIL-100(Fe).

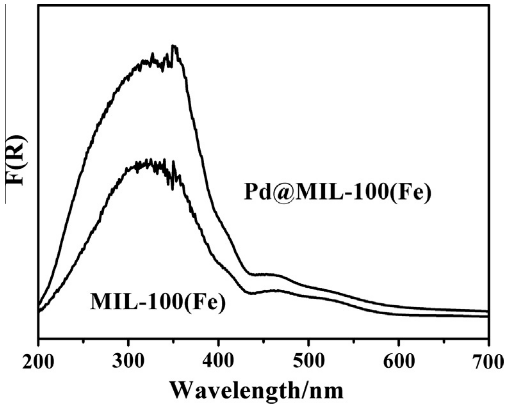

Fig. 2. UV–vis spectra of MIL-100(Fe) and Pd@MIL-100(Fe).

the light-induced N-alkylation of aniline with benzyl alcohol as compared with Pd/Fe_2O_3 and Pd/TiO_2. Only 26% of aniline was converted and 19% yield to N-benzylaniline was achieved over Pd/Fe_2O_3 after irradiation for 24 h, while no conversion of aniline was observed over visible-light-irradiated Pd/TiO_2 (Table 1, entries 12–13).

The time-dependent conversion of aniline and the formation of the products over Pd@MIL-100(Fe) was also investigated (Fig. 4a). The yield of 3a as well as of the byproducts benzaldehyde and 3b increased in the first 8 h. After that, although the yield of 3a and benzaldehyde still increased steadily, the yield to 3b decreased. This result confirms that the reaction between aniline and benzyl alcohol to produce 3a over irradiated Pd@MIL-100(Fe) also proceeds through the imine as intermediate.

The observation that the amount of 3b in the reaction system remained at a relatively low level during the whole reaction process implies that the generation of 3b is more difficult as compared with its hydrogenation to produce 3a (Fig. 4a). This assumption is not consistent with that proposed previously, which suggests that the whole N-alkylation reaction is limited by the imine hydrogenation step [14–18]. To gain more insight into this, the kinetic isotope effect (KIE) was examined using benzyl alcohol-α,α-d_2 ($C_6H_5CD_2$-OH) as an isotopic label in the alkylation reaction. The KIE (defined as k_H/k_D, in which k_H and k_D are the rate constants for the alkylation reaction using $C_6H_5CH_2OH$ and $C_6H_5CD_2OH$ as alkylating agent, respectively) was determined to be 2.6 (Fig. S3a). This value is close to the KIE value (2.8) obtained for the dehydrogenation of benzyl alcohol over Pd@MIL-100(Fe) (Fig. S3b), suggesting that the dehydrogenation of benzyl alcohol is the rate-limiting step for light-induced N-alkylation over Pd@MIL-100(Fe). The dehydrogenation of benzyl alcohol is more difficult over Pd@MIL-100(Fe) than the condensation between aniline and benzaldehyde or the hydrogenation of 3b can also be confirmed from the following controlled experiments. Only 23% of benzyl alcohol was converted to benzaldehyde over irradiated Pd@MIL-100(Fe) in 12 h. However, the condensation between aniline and benzaldehyde gave an almost quantitative transformation of aniline to 3b, and the reaction between 3b and H_2 gave a high yield of 93% to 3a under otherwise similar condition. The H_2-pretreated Pd@MIL-100(Fe) also showed catalytic activity for hydrogenation of 3b under N_2 atmosphere, with a yield of 14% to 3a. No reaction occurred in absence of Pd@MIL-100(Fe) either in the dehydrogenation of benzyl alcohol or the hydrogenation of 3b with H_2. These results confirm that the N-alkylation of amines with alcohols over Pd@MIL-100(Fe) follows a hydrogen autotransfer mechanism, with aldehydes and imines as intermediates.

Based on these observations, the light-induced N-alkylation of aniline by benzyl alcohol over Pd@MIL-100(Fe) can be proposed as follows. MOFs can be excited like conventional semiconductor photocatalysts when irradiated to generate electrons and holes. Loading of noble metals onto MOFs can result in efficient electron transfer from the excited MOFs to noble metals with lower Fermi

Table 1
Light-induced catalytic performance for the N-alkylation of aniline with benzyl alcohol under varied conditions.

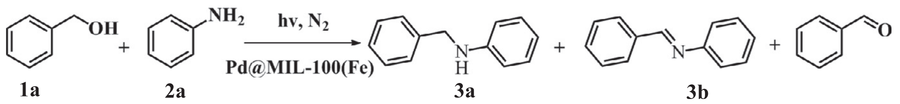

Entry	1a/2a ratio	Amine conv. (%)	Yield (%)		Aldehyde (μmol)
			3a	3b	
1[a]	1:1	–[c]	–	–	–
2[b]	1:1	–	–	–	–
3	1:1	20	5	14	12
4	1:5	45	21	23	25
5	1:10	65	42	20	21
6	1:30	88	76	11	30
7	1:50	74	53	19	41
8	1:100	49	23	24	52
9[d]	1:30	>99	86	13	45
10[e]	1:30	–	–	–	–
11[f]	1:30	56	40	15	18
12[g]	1:30	26	19	7	8
13[h]	1:30	2	–	1	2
14[i]	1:30	30	26	4	10

Notes: Reaction conditions: aniline (0.1 mmol), benzyl alcohol, CH_3CN (2 mL), Pd@MIL-100(Fe) (10 mg), N_2, light irradiation ($800\ \text{nm} \geqslant \lambda \geqslant 420\ \text{nm}$), 24 h.

[a] No catalyst.

[b] Without light irradiation.

[c] – refers to no products or negligible products detected.

[d] Irradiated for 32 h.

[e] MIL-100(Fe) instead of Pd@MIL-100(Fe) was used as catalyst.

[f] The catalyst was filtered after being irradiated for 12 h.

[g] Pd/Fe_2O_3 used as catalyst.

[h] Pd/TiO_2 used as catalyst.

[i] Pd/MIL-100(Fe) used as catalyst.

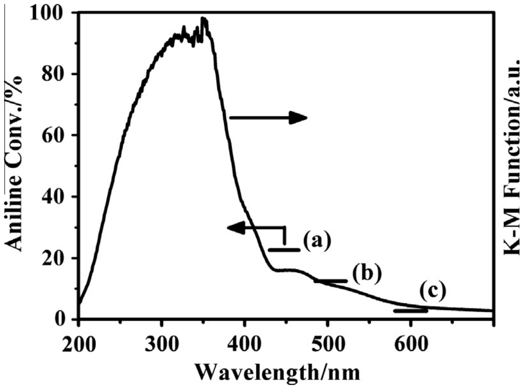

Fig. 3. Dependence of the conversion of aniline on the wavelength of incident light and the UV–vis spectra of Pd@MIL-100(Fe). The wavelength region of irradiated light was controlled using three different bandpass filters: (a) 430–465 nm; (b) 485–522 nm; (c) 581–619 nm.

levels [78]. As shown in Scheme 1, when Pd@MIL-100(Fe) was irradiated, the photogenerated electrons were transferred to Pd nanoparticles to form electron-rich Pd species (step i). The benzyl alcohol introduced into the reaction system can be activated and donates an electron to MIL-100(Fe) to form an alkoxide intermediate (step ii), which further undergoes a cleavage of the C–H bond to form benzaldehyde. Such oxidant-free formation of benzaldehyde from dehydrogenation of benzyl alcohol was previously reported over hydrotalcite-supported gold catalyst [79]. In the meantime, the hydrogen transfers to the electron-rich Pd to generate Pd hydride (step iii). The condensation between the in situ generated benzaldehyde and aniline is promoted by Lewis acidic Fe^{3+} in MIL-100(Fe) to produce imine as an intermediate (steps iv and v), which are further hydrogenated by the active Pd hydrides to generate N-alkyl amine (step vi).

To investigate the substrate scope of this reaction, different functional substituted anilines were used to carry out the alkylation reactions (Table 2). Except for *p*-nitroaniline, all the investigated aromatic amines can be transformed to the corresponding N-alkyl anilines after irradiation for 24 h, but with different yields. Aniline with electron-withdrawing substituents such as –Cl showed significantly decreased conversion ratios (18%) and low yields of N-benzyl-4-chloroaniline (11%) (Table 2, entry 2), while those with electron-donating groups ($–OCH_3$ and $–CH_3$) exhibited slightly increased conversion ratios (90–92%) and comparable yields to N-alkyl amine (73-77%) (Table 2, entries 4–5). The reactions between benzyl alcohols with different substituents and aniline also proceeded efficiently over Pd@MIL-100(Fe), except for p-nitrobenzyl alcohol. Medium to high conversion ratios of aniline (72–85%) and reasonable yields of N-alkyl amines (51–70%) were realized after irradiation for 24 h (Table 2, entries 6–9). The observation that substrates with different substituents on their phenyl rings showed varied activities suggests the existence of an electronic effect. This is reasonable, since the nucleophilic attack toward the aldehydes by the aniline is an important step in this reaction. Pd@MIL-100(Fe) was inactive for the reaction between aniline and *p*-nitrobenzyl alcohol or that between *p*-nitroaniline and benzyl alcohol (Table 2, entries 3 and 10). It is probable that the adsorption of the strong electron-withdrawing $–NO_2$ group onto the surfaces of the electron-rich Pd nanoparticles would impede hydrogen transfer to the Pd species to form Pd hydride.

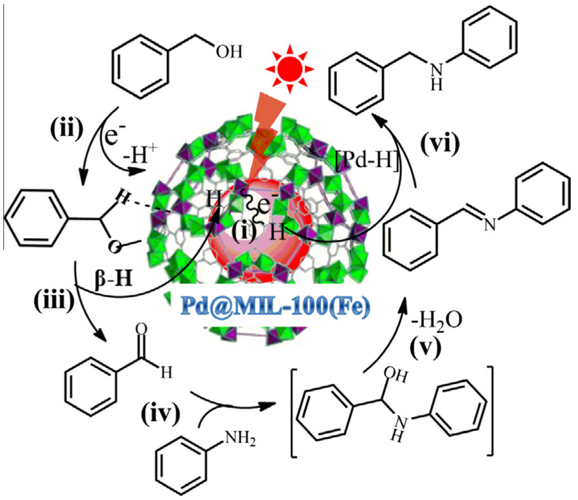

Scheme 1. Proposed mechanism for N-alkylation of aniline with benzyl alcohol via hydrogen autotransfer process over Pd@MIL-100(Fe).

The scope of the substrates can also be expanded to aliphatic amines and alcohols (Table 2, entries 11–14). Either the reactions of aliphatic amines with benzyl alcohols or those between anilines and aliphatic alcohols occurred over the current Pd@MIL-100(Fe), but with a lower conversion ratio (13–55%) and lower yield (8–43%) than their respective N-alkyl amines.

Pd@MIL-100(Fe) showed high stability for the light-induced N-alkylation reaction. No obvious loss of the activity was observed after five cycling tests (Fig. 5). ICP analysis of the filtrate revealed no detectable Pd and Fe. The Pd@MIL-100(Fe) after five runs showed similar XRD patterns and its specific surface area ($1392\ m^2\ g^{-1}$) is comparable to that of the fresh one ($1562\ m^2\ g^{-1}$) (Figs. S4–S5). In addition, the TEM image of the used catalyst shows that Pd nanoparticles with almost similar size distributions were maintained (Fig. S6a).

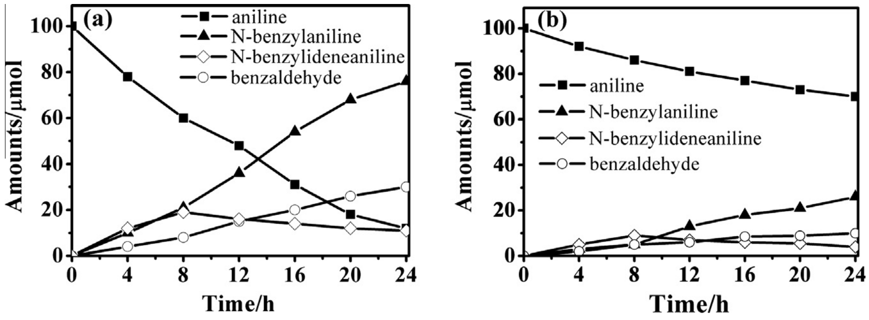

Fig. 4. Time-dependent changes in the amounts of aniline and the three products during N-alkylation of aniline with benzyl alcohol under visible light irradiation over (a) Pd@MIL-100(Fe) and (b) Pd/MIL-100(Fe). The ratio of Pd to aniline is 1:100.

Table 2
Light-induced catalytic performance for N-alkylation of amines with alcohols over Pd@MIL-100(Fe).

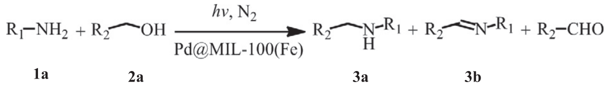

Entry	Substrates		Amine conv. (%)	Yield (%)		Aldehyde (μmol)
	1a	2a		3a	3b	
1	Aniline	Benzyl alcohol	88	76	11	30
2	*p*-Chloroaniline	Benzyl alcohol	18	11	7	40
3	*p*-Nitroaniline	Benzyl alcohol	10	–	8	54
4	*p*-Methoxyaniline	Benzyl alcohol	90	73	15	25
5	*p*-Touidine	Benzyl alcohol	92	77	13	23
6	Aniline	*p*-Methoxybenzyl alcohol	81	63	18	28
7	Aniline	*p*-Methylbenzyl alcohol	85	70	13	30
8	Aniline	*m*-Methylbenzyl alcohol	78	62	16	24
9	Aniline	*o*-Methylbenzyl alcohol	72	51	20	20
10	Aniline	*p*-Nitrobenzyl alcohol	6	-	6	5
11	Cyclohexylamine	Benzyl alcohol	55	43	11	21
12	*n*-Butylamine	Benzyl alcohol	34	20	14	27
13	Aniline	Cyclohexanol	18	11	6	12
14	Aniline	Butyl alcohol	13	8	4	8

Notes: Reaction conditions: amine (0.1 mmol), alcohol (3 mmol), CH_3CN (2 mL), catalyst (10 mg), N_2, light irradiation (800 nm $\geqslant \lambda \geqslant$ 420 nm), 24 h.

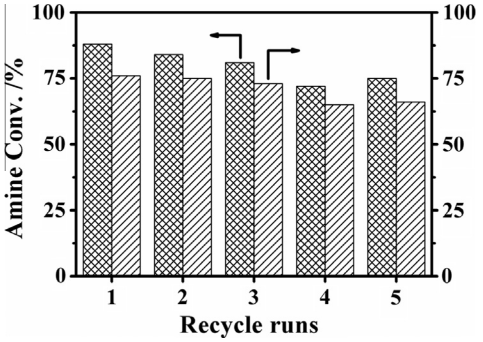

Fig. 5. Cycling of Pd@MIL-100(Fe) for the N-alkylation of aniline with benzyl alcohol under visible light irradiation. Each run was irradiated for 24 h.

For comparison, Pd nanoparticles deposited on the external surface of MIL-100(Fe) (Pd/MIL-100(Fe)) were also prepared via a conventional single-solvent impregnation followed by a similar photoreduction process and was used in the reaction between aniline and benzyl alcohol. TEM/HRTEM images of Pd/MIL-100(Fe) show that Pd nanoparticles at a size of 6–12 nm were deposited on the surface of MIL-100(Fe) (Figs. 1e, f, and S7). It was found that Pd/MIL-100(Fe) exhibited inferior catalytic activity for the N-alkylation reaction to Pd@MIL-100(Fe) under similar conditions (Fig. 4b). Only about 30% of aniline was converted and a lower yield of 3a (26%) was achieved over Pd/MIL-100(Fe) after irradiation for 24 h (Table 1, entry 14). The lower activity for N-alkylation over Pd/MIL-100(Fe) can be attributed to its inferior activity for alcohol dehydrogenation, since the conversion of benzyl alcohol to benzaldehyde over Pd@MIL-100(Fe) (23%) was much higher than that over Pd/MIL-100(Fe) (7.7%) in a similar irradiation time (12 h). It is believed that due to their small size, the cavity-encapsulated Pd nanoparticles contain more active unsaturated Pd atoms than those supported on the surface of MIL-100(Fe), and the dehydrogenation of alcohol to generate aldehydes, which proceeds via the cleavage of the C–H bond, is catalyzed by Pd nanoparticles. In addition, with the cavities of the MIL-100(Fe) acting as nanoreactors, the encapsulated Pd nanoparticles and the substrates confined in close proximity can ensure a rapid electron transfer from the excited Fe–O clusters to Pd nanoparticles, which favors the activation of the substrates to realize an efficient light-induced multistep reaction. It was also found that Pd/MIL-100(Fe) showed poor stability, as evidenced from the decreased activity during the cycling reactions (Fig. S8). Although the used Pd/MIL-100(Fe) showed XRD patterns similar to those of the fresh Pd/MIL-100 (Fe), its TEM image shows larger Pd nanoparticles (10–15 nm), implying that Pd nanoparticles aggregated during the reaction (Figs. S6b and S9).

4. Conclusions

In summary, Pd@MIL-100(Fe), with Pd nanoparticles confined inside the cavities of MIL-100(Fe), was successfully obtained via double-solvent impregnation combined with a photoreduction approach and acted as a superior catalyst for the light-induced N-alkylation reaction of amines by alcohols. This is the first demonstration of M/MOFs nanocomposite catalysts for the light-induced N-alkylation of amines with alcohols. This study not only provides a green method for the production of N-alkyl amines, but also highlights the great potential of using MOFs for light-induced organic syntheses. It is anticipated that the combination of the diversified MOFs and the metal nanoparticles will bring about almost infinite possibilities for developing multifunctional catalysts for light-induced organic transformations.

Acknowledgments

This work was supported by the 973 Program (2014CB239303), the NSFC (21273035), the Specialized Research Fund for the Doctoral Program of Higher Education (20123514110002), and an Independent Research Project of State Key Laboratory of Photocatalysis on Energy and Environment (2014A03). Z. Li thanks the Award Program for Minjiang Scholar Professorship for financial support. We also thank Professor Masakazu Anpo for helpful discussions.

Appendix A. Supplementary material

Supplementary data associated with this article can be found, in the online version, at http://dx.doi.org/10.1016/j.jcat.2016.07.021.

References

[1] S.A. Lawrence, Amines: Synthesis, Properties, and Application, Cambridge University Press, Cambridge, 2006.
[2] R.N. Salvatore, C.H. Yoon, K.W. Jung, Tetrahedron 57 (2001) 7785.

[3] G. Guillena, D.J. Ramón, M. Yus, Chem. Rev. 110 (2010) 1611.
[4] M. Ousmane, G. Perrussel, Z. Yan, J.-M. Clacens, F. De Campo, M. Pera-Titus, J. Catal. 309 (2014) 439.
[5] S. Sithambaram, R. Kumar, Y.-C. Son, S.L. Suib, J. Catal. 253 (2008) 269.
[6] M.H.S.A. Hamid, C.L. Allen, G.W. Lamb, A.C. Maxwell, H.C. Maytum, A.J.A. Watson, J.M.J. Williams, J. Am. Chem. Soc. 131 (2009) 1766.
[7] Q. Yang, Q.F. Wang, Z.K. Yu, Chem. Soc. Rev. 44 (2015) 2305.
[8] A. Corma, T. Ródenas, M.J. Sabater, Chem. Eur. J. 16 (2010) 254.
[9] O. Saidi, A.J. Blacker, M.M. Farah, S.P. Marsden, J.M.J. Williams, Chem. Commun. 46 (2010) 1541.
[10] J.W. Kim, K. Yamaguchi, N. Mizuno, J. Catal. 263 (2009) 205.
[11] S. Röler, M. Ertl, T. Irrgang, R. Kempe, Angew. Chem. Int. Ed. 54 (2015) 15046.
[12] C. Gunanathan, D. Milstein, Acc. Chem. Res. 44 (2011) 588.
[13] T. Ishida, N. Kawakita, T. Akita, M. Haruta, Gold Bull. 42 (2009) 267.
[14] A. Nandakumar, S.P. Midya, V.G. Landge, E. Balaraman, Angew. Chem. Int. Ed. 54 (2015) 11022.
[15] Y.S. Zhao, S.W. Foo, S. Saito, Angew. Chem. Int. Ed. 50 (2011) 3006.
[16] H.H. Liu, G.-K. Chuah, S. Jaenicke, J. Catal. 292 (2012) 130.
[17] Y. Zhang, C.-S. Lim, D.S.B. Sim, H.-J. Pan, Y. Zhao, Angew. Chem. Int. Ed. 53 (2014) 1399.
[18] Y. Shiraishi, K. Fujiwara, Y. Sugano, S. Ichikawa, T. Hirai, ACS Catal. 3 (2013) 312.
[19] L.N. Zhang, Y. Zhang, Y.Q. Deng, F. Shi, Catal. Sci. Technol. 5 (2015) 3226.
[20] D. Stíbal, J. Jacinto Sá, J.A.V. Bokhoven, Catal. Sci. Technol. 3 (2013) 94.
[21] J.W. Liu, L.F. Chen, H. Cui, J.H. Zhang, L. Zhang, C.-Y. Su, Chem. Soc. Rev. 42 (2014) 6011.
[22] A. Stein, Adv. Mater. 15 (2003) 763.
[23] T. Uemura, N. Yanai, S. Kitagawa, Chem. Soc. Rev. 38 (2009) 1228.
[24] N. Yi, Y. Cao, Y. Su, W.-L. Dai, H.-Y. He, K.-N. Fan, J. Catal. 230 (2005) 249.
[25] J.J. Zhou, P. Wang, C.X. Wang, Y.T. Goh, Z. Fang, P.B. Messersmith, H.W. Duan, ACS Nano 9 (2015) 6951.
[26] Y.-H. Kang, X.-D. Liu, N. Yan, Y. Jiang, X.-Q. Liu, L.-B. Sun, J.-R. Li, J. Am. Chem. Soc. 138 (2016) 6099.
[27] G. Lu, S.Z. Li, Z. Guo, O.K. Farha, B.G. Hauser, X.Y. Qi, Y. Wang, X. Wang, S.Y. Han, X.G. Liu, J.S. DuChene, H. Zhang, Q.C. Zhang, X.D. Chen, J. Ma, S.C.J. Loo, W.D. Wei, Y.H. Yang, J.T. Hupp, F.W. Huo, Nat. Chem. 4 (2012) 310.
[28] L.Y. Chen, H.R. Chen, R. Luque, Y.W. Li, Chem. Sci. 5 (2014) 3708.
[29] Y.J. Cui, Y.F. Yue, G.D. Qian, B.L. Chen, Chem. Rev. 112 (2012) 1126.
[30] W.-Y. Gao, M. Chrzanowski, S.Q. Ma, Chem. Soc. Rev. 43 (2014) 5841.
[31] H.-C. Zhou, S. Kitagawa, Chem. Soc. Rev. 43 (2014) 5415.
[32] W.M. Xuan, C.F. Zhu, Y. Liu, Y. Cui, Chem. Soc. Rev. 41 (2012) 1677.
[33] A. Corma, H. García, F.X. Llabrés i Xamena, Chem. Rev. 110 (2010) 4606.
[34] O. Shekhah, J. Liu, R.A. Fischer, Ch. Wöll, Chem. Soc. Rev. 40 (2011) 1081.
[35] J.Y. Lee, O.K. Farha, J. Roberts, K.A. Scheidt, S.T. Nguyen, J.T. Hupp, Chem. Soc. Rev. 38 (2009) 1450.
[36] S.M. Cohen, Chem. Rev. 112 (2012) 970.
[37] S.L. Qiu, M. Xue, G.S. Zhu, Chem. Soc. Rev. 43 (2014) 6116.
[38] Q.-L. Zhu, Q. Xu, Chem. Soc. Rev. 43 (2014) 5468.
[39] H.R. Moon, D.-W. Lim, M.P. Suh, Chem. Soc. Rev. 42 (2013) 1807.
[40] H.-L. Jiang, Q. Xu, Chem. Commun. 47 (2011) 3351.
[41] H. Furukawa, U. Müller, O.M. Yaghi, Angew. Chem. Int. Ed. 54 (2015) 3417.
[42] Z.Q. Wang, S.M. Cohen, Chem. Soc. Rev. 38 (2009) 1315.
[43] W.N. Zhang, G. Lu, C.L. Cui, Y.Y. Liu, S.Z. Li, W.J. Yan, C. Xing, Y.R. Chi, Y.H. Yang, F.W. Huo, Adv. Mater. 26 (2014) 4056.
[44] Y.K. Hwang, D.-Y. Hong, J.-S. Chang, S.H. Jhung, Y.-K. Seo, J. Kim, A. Vimont, M. Daturi, C. Serre, G. Férey, Angew. Chem. Int. Ed. 47 (2008) 4144.
[45] A. Dhakshinamoorthy, H. Garcia, Chem. Soc. Rev. 41 (2012) 5262.
[46] A.H. Chughtai, N. Ahmad, H.A. Younus, A. Laypkov, F. Verpoort, Chem. Soc. Rev. 44 (2015) 6804.
[47] L.Y. Chen, B.B. Huang, X. Qiu, X. Wang, R. Luque, Y.W. Li, Chem. Sci. 7 (2016) 228.
[48] X.L. Li, Z.Y. Guo, C.X. Xiao, T.W. Goh, D. Tesfagaber, W.Y. Huang, ACS Catal. 4 (2014) 3490.
[49] P. Hester, S.J. Xu, W. Liang, N. Al-Janabi, R. Vakili, P. Hill, C.A. Muryn, X.B. Chen, P.A. Martin, X.L. Fan, J. Catal. 340 (2016) 85.
[50] J. Juan-Alcañiz, J. Ferrando-Soria, I. Luz, P. Serra-Crespo, E. Skupien, V.P. Santos, E. Pardo, F.X. Llabrés i Xamena, F. Kapteijn, J. Gascon, J. Catal. 307 (2013) 295.
[51] Z.C. Zhang, Y.F. Chen, X.B. Xu, J.C. Zhang, G.L. Xiang, W. He, X. Wang, Angew. Chem. Int. Ed. 53 (2014) 429.
[52] Y.B. Huang, S.J. Liu, Z.J. Lin, W.J. Li, X.F. Li, R. Cao, J. Catal. 292 (2012) 111.
[53] Y.L. Liu, Z.Y. Tang, Adv. Mater. 25 (2013) 5819.
[54] A. Aijaz, Q. Xu, J. Phys. Chem. Lett. 5 (2014) 1400.
[55] X.J. Lang, X.D. Chen, J.C. Zhao, Chem. Soc. Rev. 43 (2014) 473.
[56] H. Tong, S.X. Ouyang, Y.P. Bi, N. Umezawa, M. Oshikiri, J.H. Ye, Adv. Mater. 24 (2012) 229.
[57] W.G. Tu, Y. Zhou, Z.G. Zou, Adv. Mater. 26 (2014) 4607.
[58] T. Zhang, W.B. Lin, Chem. Soc. Rev. 43 (2014) 5982.
[59] D.K. Wang, R.K. Huang, W.J. Liu, D.R. Sun, Z.H. Li, ACS Catal. 4 (2014) 4254.
[60] Y.H. Fu, D.R. Sun, Y.J. Chen, R.K. Huang, Z.X. Ding, X.Z. Fu, Z.H. Li, Angew. Chem. Int. Ed. 51 (2012) 3364.
[61] M.A. Nasalevich, M. van der Veen, F. Kapteijn, J. Gascon, CrystEngComm 16 (2014) 4919.
[62] M. Alvaro, E. Carbonell, B. Ferrer, F.X. Llabrés i Xamena, H. Garcia, Chem. Eur. J. 13 (2007) 5106.
[63] T. Tachikawa, J.R. Choi, M. Fujitsuka, T. Majima, J. Phys. Chem. C 112 (2008) 14090.
[64] D.S. Sun, W.J. Liu, M. Qiu, Y.F. Zhang, Z.H. Li, Chem. Commun. 51 (2015) 2056.
[65] D.K. Wang, Z.H. Li, Catal. Sci. Technol. 5 (2015) 1623.
[66] J.-L.T.H. Zhou, Y.H. Du, A. Borgna, J.D. Hong, Y.B. Wang, J.Y. Han, W. Zhang, R. Xu, Energy Environ. Sci. 6 (2013) 3229.
[67] S.Y. Jin, H.-J. Son, O.K. Farha, G.P. Wiederrecht, J.T. Hupp, J. Am. Chem. Soc. 135 (2013) 955.
[68] V. Stavila, A.A. Talin, M.D. Allendorf, Chem. Soc. Rev. 43 (2014) 5994.
[69] Z.C. Hu, B.J. Deibert, J. Li, Chem. Soc. Rev. 43 (2014) 5815.
[70] S. Natarajan, P. Mahata, Chem. Soc. Rev. 38 (2009) 2304.
[71] P. Horcajada, S. Surblé, C. Serre, D.-Y. Hong, Y.-K. Seo, J.-S. Chang, J.-M. Grenèche, I. Margiolaki, G. Férey, Chem. Commun. (2007) 2820.
[72] D.K. Wang, M.T. Wang, Z.H. Li, ACS Catal. 5 (2015) 6852.
[73] K.G.M. Laurier, F. Vermoortele, R. Ameloot, D.E. De Vos, J. Hofkens, M.B.J. Roeffaers, J. Am. Chem. Soc. 135 (2013) 14488.
[74] J.-W. Zhang, H.-T. Zhang, Z.-Y. Du, X.Q. Wang, S.-H. Yu, H.-L. Jiang, Chem. Commun. 50 (2014) 1092.
[75] Q.-L. Zhu, J. Li, Q. Xu, J. Am. Chem. Soc. 135 (2013) 10210.
[76] A. Aijaz, A. Karkamkar, Y.J. Choi, N. Tsumori, E. Rönnebro, T. Autrey, H. Shioyama, Q. Xu, J. Am. Chem. Soc. 134 (2012) 13926.
[77] X.M. Chen, G.H. Wu, J.M. Chen, X. Chen, Z.X. Xie, X.R. Wang, J. Am. Chem. Soc. 133 (2011) 3693.
[78] D.R. Sun, W.J. Liu, Y.H. Fu, Z.X. Fang, F.X. Sun, X.Z. Fu, Y.F. Zhang, Z.H. Li, Chem. Eur. J. 20 (2014) 4780.
[79] W.H. Fang, J.S. Chen, Q.H. Zhang, W.P. Deng, Y. Wang, Chem. Eur. J. 17 (2011) 1247.